



Cavity spin twisting in coherent population trapping

Xiangming Hu ^{*}, Chengdeng Gou, and Jun Xu 

College of Physical Science and Technology, Central China Normal University, Wuhan 430079, People's Republic of China



(Received 4 September 2023; revised 24 June 2024; accepted 3 July 2024; published 22 July 2024)

Spin twisting is generally not incompatible with steady-state atomic coherence because spin twisting as a representative kind of parametric processes is based on far-off-resonant atom-field interactions while the steady-state atomic coherence is achieved mainly by resonant interactions. Here we propose a resonant plus far-off-resonant scheme to generate the compatibility. The resonant part uses coherent population trapping (CPT) for steady-state maximal atomic coherence, while the far-off-resonant part utilizes Stark shift for a nonlinear response in analog with the motion of a cavity mirror under radiation pressure. The compatible combination CPT with the spin optodynamics analog to cavity optomechanics leads to the spin one- or two-axis-twisting together with steady-state maximal atomic coherence. The general conditions and the parameter regimes for the compatibility are analyzed. This scheme illustrates that the combination of CPT with Stark shift provides an efficient way for the compatibility of the spin twisting squeezing with steady-state maximal atomic coherence.

DOI: [10.1103/PhysRevA.110.013709](https://doi.org/10.1103/PhysRevA.110.013709)

I. INTRODUCTION

Squeezed spin states [1–4] have applications in so many fields such as Ramsey spectroscopy [1–4], atomic clocks [2,3], gravitational wave interferometers [5–7], and quantum information processing [8–11]. There are two representative squeezing mechanisms [1–4], which are respectively referred to as one-axis-twisting (OAT) $\hat{H} \propto \hat{J}_y^2$ or $\hat{H} \propto \hat{J}_z^2$, and two-axis-twisting (TAT) $\hat{H} \propto \hat{J}_y^2 - \hat{J}_z^2$, where (\hat{J}_y, \hat{J}_z) are zero-mean components orthogonal to the total mean $J = J_x$. These two mechanisms, which are suited for a pair of ground states, are established through the dispersive atom-field interactions in Λ configuration [12–26]. An initial spin coherent state is prepared by optically pumping the atoms into a ground state and then by applying a microwave $\pi/2$ pulse to yield the J_x component as the total mean spin $J = J_x$. Then an evolution into the spin squeezed states is usually performed by using optical π pulses [15–18].

The spin twisting as a large type of parametric processes since it is based on far off-resonant atom-field interactions, is generally not coexistent with steady-state large or maximal atomic coherence, which is usually based on resonant or near-resonant interactions. The large or maximal atomic coherence is just highly demanded for quantum manipulation, such as single photon swap gate [27], efficient nonlinear frequency conversion [28–31], and storage and retrieval of coherent optical information [32]. We propose a resonant plus far-off-resonant scheme.

On one hand, the resonant part is based on coherent population trapping (CPT) [33] and used to yield steady-state maximal atomic coherence. When two beams of lasers couple two atomic ground states to a common excited state in Λ configuration, the atoms are trapped in a coherent superposition

(dark state) of the ground states. Since the atoms stay in the dark state, fluorescence disappears. Within the CPT window, the absorption and the fluorescence emission remains negligibly weak, and in contrast, the dispersive nonlinearity is remarkably strong. As is well known, CPT underlines a wealth of related phenomena such as electromagnetically induced transparency [34–37], laser without inversion [38–41], magnetometry [42], nonlinear optics at low light levels [37], and atomic spin squeezing [36,37,43]. Here we use CPT for steady-state maximal level coherence and interferingly eliminating spontaneous emission.

On the other hand, the far-off-resonant part is relied on Stark shift and acts as spin optodynamics analogous to cavity optomechanics. Cavity optomechanics has arisen as a fascinating field controlling macroscopic mechanical objects at the quantum limit [44]. The position change of a mechanical oscillator by radiation pressure gives an increment to the frequency of cavity photons. Various phenomena emerge, including ponderomotive optical squeezing [45], quantum-limited measurements [46], cavity cooling [47,48], and mechanical response to photon shot noise [49]. In terms of bare atomic states, an analog of spin optodynamics to cavity optomechanics was proposed by Brahm and Stamper-Kurn [50], who used an ac Stark shift in the absence of resonant interaction. In the present scheme, we introduce the ac Stark shift into the CPT resonant system. In this setting, we construct a CPT based cavity spin optodynamics and exploit the similarities between CPT based spins and harmonic oscillators [51]. The Stark shift interaction of the ground state spin with the cavity field turns out to take an analog of the cavity optomechanics in terms of the dark state.

The compatible combination of CPT resonance with spin optomechanics analog drives the system into a steady state, in which spin OAT or TAT (or general twisting between them) is coexistent with the maximal atomic coherence as long as the applied fields persist. We performed an analytic description

^{*}Contact author: xmhu@ccnu.edu.cn

and a numerical calculation for the coexistent effects. The steady-state squeezing reaches about 50% (3 dB), which is the best degree for the noise squeezing as in the parametric processes [52,53].

The most remarkable difference of our scheme from the previous ones lies in the compatible combination of resonant interaction (CPT) with far-off-resonant interaction (Stark shift), and in the coexistence of the steady-state maximal atomic coherence with the spin twisting squeezing. Previously, to seek for the nonlinearities for the spin twisting and to avoid spontaneous emission, one resorts to far-off-resonant (purely dispersive) cases, where the atoms are hardly excited and spontaneous emission is free. However, the steady-state atomic coherence is prepared usually when resonant interactions are employed. The nonlinearities necessary for the spin twisting are spoiled when some resonant processes are involved. To performing the spin twisting squeezing mechanisms, it is necessary to prepare initially the coherent spin states by using microwave pulses. In a surprising contrast, in our scheme, there is no need to prepare the initial coherent spin states. Specifically, it is no longer necessary to prepare initially the large or maximal atomic coherence. As the system evolves into the steady state, the resonant part (CPT) maintains the atomic dark state and gives the steady-state maximal atomic coherence and the far-off-resonant part (spin optomechanics analog) induces the OAT or TAT (or general twisting between them) and yields the spin squeezing. It is the compatible combination of CPT with the spin optomechanics analog that leads to the coexistence of the spin twisting squeezing with the steady-state maximal atomic coherence.

II. STEADY-STATE MAXIMAL ATOMIC COHERENCE AND SPIN OPTOMECHANICS ANALOG

First of all, we present our model system. As shown in Fig. 1(a), an ensemble of N atoms interacts resonantly or near-resonantly with two coherent fields in Λ configuration and far off resonantly with a cavity field leading to a N configuration. The master equation is derived for the density operator $\hat{\rho}$ of the coupled system in a dipole approximation and an appropriate rotating frame as ($\hbar = 1$) [52,53]

$$\dot{\hat{\rho}} = -i[\hat{H}_{\text{CPT}} + \hat{H}_{\text{Stark}}, \hat{\rho}] + \mathcal{L}\hat{\rho}, \quad (1)$$

with

$$\begin{aligned} \hat{H}_{\text{CPT}} = & \Omega_1(\hat{J}_{13} + \hat{J}_{31}) + \Omega_2(\hat{J}_{23} + \hat{J}_{32}) + (\Delta_1 - \Delta_2)\hat{J}_{22} \\ & + \Delta_1\hat{J}_{33}, \end{aligned} \quad (2)$$

$$\begin{aligned} \hat{H}_{\text{Stark}} = & g(\hat{a}^\dagger\hat{J}_{24} + \hat{J}_{42}\hat{a}) + (\Delta_1 - \Delta_2 + \Delta_0)\hat{J}_{44} \\ & + i(\varepsilon\hat{a}^\dagger e^{i\Delta_c t} - \varepsilon^*\hat{a}e^{-i\Delta_c t}), \end{aligned} \quad (3)$$

$$\begin{aligned} \mathcal{L}\hat{\rho} = & \sum_{\mu=1}^N (\Gamma_1\mathcal{L}_{\hat{J}_{13,\mu}}\hat{\rho} + \Gamma_1\mathcal{L}_{\hat{J}_{23,\mu}}\hat{\rho} + \Gamma_2\mathcal{L}_{\hat{J}_{14,\mu}}\hat{\rho} + \Gamma_2\mathcal{L}_{\hat{J}_{24,\mu}}\hat{\rho} \\ & + \gamma_z\mathcal{L}_{\hat{J}_{z,\mu}}\hat{\rho}) + \kappa\mathcal{L}_{\hat{a}}\hat{\rho}, \end{aligned} \quad (4)$$

where \hat{H}_{CPT} , \hat{H}_{Stark} , and $\mathcal{L}\hat{\rho}$ are the CPT interaction, the atom-cavity-field interaction, and the vacuum-induced relaxation, respectively. We define $\hat{J}_{ij} = \sum_{\mu=1}^N \hat{J}_{ij,\mu}$ ($\hat{J}_{ij,\mu} =$

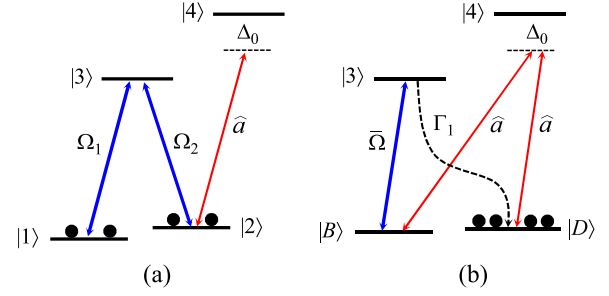


FIG. 1. Resonant plus far off-resonant atom-field interaction for spin optodynamics analog to cavity optomechanics. (a) The picture in terms of bare states ($|1\rangle$, $|2\rangle$, $|3\rangle$, $|4\rangle$). The atoms are trapped coherently in the bare state $|1\rangle$ and $|2\rangle$ by the two classical fields (Rabi frequencies $\Omega_{1,2}$) through the $|1\rangle \xleftrightarrow{\Omega_1} |3\rangle$ and $|2\rangle \xleftrightarrow{\Omega_2} |3\rangle$ transitions in Λ configuration with. Not shown in the sketch are the spontaneous transitions $|3\rangle \xrightarrow{\Gamma_1} |1, 2\rangle$ and $|4\rangle \xrightarrow{\Gamma_2} |1, 2\rangle$. The far off-resonant $|2\rangle \xleftrightarrow{\Delta_0} |4\rangle$ transition (large detuning Δ_0) with a cavity field (annihilation operator \hat{a}) is introduced for ac Stark shift (dispersive interaction). (b) The picture with the ground state superpositions ($|D\rangle$, $|B\rangle$). The dark state $|D\rangle$ collects all population while the bright state $|B\rangle$ becomes empty. CPT is performed through the successive coherent and spontaneous transitions $|B\rangle \xleftrightarrow{\bar{\Omega}} |3\rangle \xrightarrow{\Gamma_1} |D\rangle$. Raman transition between $|D\rangle$ and $|B\rangle$ through the virtual level $|4\rangle$ by the far off-resonant cavity field \hat{a} creates cavity optomechanics-like interaction [Eq. (14)].

($|i\rangle\langle j|$) $_{\mu}$, $i, j = 1, 2, 3, 4$) as the collective spin-flip ($i \neq j$) and population projection ($i = j$) operators. \hat{a} and \hat{a}^\dagger are the annihilation and creation operators, respectively, of the quantized cavity field. $\Omega_{1,2}$ are half Rabi frequencies (real) for the transitions $|1, 2\rangle \leftrightarrow |3\rangle$. g is the coupling constant between the cavity field and the atoms and ε is the amplitude of the external driving field. $\Delta_j = \omega_{j3} - \omega_j$ ($j = 1, 2$) and $\Delta_0 = \omega_{24} - \omega_c$ are the atom-field detunings, $\omega_{1,2}$ are the frequencies of the CPT fields, ω_c is the cavity field frequency. $\Delta_c = \omega_c - \omega_0$ is the cavity detuning from the external driving field frequency ω_0 . $\mathcal{L}_{\hat{\rho}}$ in the relaxation term $\mathcal{L}\hat{\rho}$ takes the form with $\mathcal{L}_{\hat{\rho}} = \hat{\rho}\hat{\rho}^\dagger - \frac{1}{2}\hat{\rho}^\dagger\hat{\rho} - \frac{1}{2}\hat{\rho}\hat{\rho}^\dagger$, $\hat{J}_{z,\mu} = \hat{J}_{22,\mu} - \hat{J}_{11,\mu}$. Γ_1 (Γ_2) is the rate of spontaneous emission from the excited state $|3\rangle$ ($|4\rangle$) to the ground state $|1\rangle$ and $|2\rangle$, respectively, γ_z is the dephasing rate of the ground state $|1\rangle$ and $|2\rangle$ and κ is the rate of the cavity loss. For cold atoms the phase damping is negligibly weak compared with the atomic and cavity decay rates: $\gamma_z \sim (10^{-4} \sim 10^{-3})(\Gamma_{1,2}, \kappa) \ll (\Gamma_{1,2}, \kappa)$.

The present model consists of CPT effect and Stark shift as its two compatible parts. Let's describe first the CPT effect due to the driving fields ($\Omega_{1,2}$). In terms of a pair of superposition states [33–37]

$$\begin{aligned} |D\rangle &= \frac{1}{\bar{\Omega}}(-\Omega_2|1\rangle + \Omega_1|2\rangle), \\ |B\rangle &= \frac{1}{\bar{\Omega}}(\Omega_1|1\rangle + \Omega_2|2\rangle), \end{aligned} \quad (5)$$

where $\bar{\Omega} = \sqrt{\Omega_1^2 + \Omega_2^2}$. In the case of two-photon resonance ($\Delta_1 = \Delta_2 = \Delta$), Hamiltonian (2) takes a simple form

$$\hat{H}_{\text{CPT}} = \bar{\Omega}(\hat{J}_{B3} + \hat{J}_{3B}) + \Delta\hat{J}_{33}, \quad (6)$$

in which the $|D\rangle$ state is decoupled and $\bar{\Omega}$ acts as an effective field. As shown in Fig. 1(b), through the successive coherent and spontaneous transitions $|B\rangle \xrightarrow{\bar{\Omega}} |3\rangle \xrightarrow{\Gamma_1} |D\rangle$, the atoms are only transferred into the $|D\rangle$ state but not out of it. In the absence of the cavity field ($ga = 0$), to the first order in γ_z/Γ_1 , we easily obtain steady-state solutions such as

$$J_{DD} = N \left[1 - \frac{2\gamma_z}{\Gamma_1} \left(1 + \frac{\Gamma_1^2 + \Delta^2}{2\bar{\Omega}^2} \right) \right], \quad (7)$$

where and from now on we denote the mean value of any operator by removing the hat on it. Since the phase damping is negligibly weak ($\gamma_z/\Gamma_1 \rightarrow 0$), so long as $\Delta/\bar{\Omega}$ is not too large we have

$$J_{DD} = N, \quad J_{ij} = 0 \quad (i, j = D, B, 3; ij \neq DD), \quad (8)$$

which indicates clearly that the atoms are trapped in the $|D\rangle$ state while both $|B\rangle$ and $|3\rangle$ states are empty. The $|D\rangle$ state is usually named the ‘‘dark state,’’ while the $|B\rangle$ state is called the ‘‘bright state.’’ The atoms, since they stay in the $|D\rangle$ state as a coherent superposition of the $|1\rangle$ and $|2\rangle$ states, essentially flip only forward and back between them. This is just the so-called ‘‘dark resonance.’’ Using the reverse transform of Eq. (5), we can obtain the atomic populations and coherence in terms of the bare states ($|1\rangle, |2\rangle, |3\rangle$). For $\Omega_1 = \Omega_2 = \Omega$ we have

$$J_{11} = J_{22} = \frac{N}{2}, \quad J_{12} = -\frac{N}{2}, \quad (9)$$

which indicates the maximal atomic coherence between the ground states when CPT happens.

For convenience we define the Cartesian components ($\hat{J}_x, \hat{J}_y, \hat{J}_z$) using single letter axis names as the subscripts and discriminating the flip and projection operators with two atomic level letters as subscripts

$$\begin{aligned} \hat{J}_x &\equiv -(\hat{J}_{12} + \hat{J}_{21}) = \hat{J}_{DD} - \hat{J}_{BB}, \\ \hat{J}_y &\equiv -i(\hat{J}_{12} - \hat{J}_{21}) = i(\hat{J}_{DB} - \hat{J}_{BD}), \\ \hat{J}_z &\equiv \hat{J}_{22} - \hat{J}_{11} = \hat{J}_{DB} + \hat{J}_{BD}. \end{aligned} \quad (10)$$

Using Eqs. (8) or (9) we express the means of the Cartesian components

$$J_x = N, \quad J_y = J_z = 0. \quad (11)$$

Next we turn to the Stark shift due to the cavity field ($ga \neq 0$). Eliminating the excited state $|4\rangle$ and using the equal detunings $\Delta_1 = \Delta_2 = \Delta$ for CPT, we simplify the interaction Hamiltonian \hat{H}_{Stark} in Eq. (3) to

$$\hat{H}_{\text{Stark}} = -\frac{g^2}{\Delta_0} \hat{a}^\dagger \hat{a} \hat{J}_{22} + i(\varepsilon \hat{a}^\dagger e^{i\Delta_0 t} - \varepsilon^* \hat{a} e^{-i\Delta_0 t}). \quad (12)$$

The first term indicates the atomic state $|2\rangle$ shift $-(g^2/\Delta_0)a^*a$ by the cavity and the cavity field frequency shift $-(g^2/\Delta_0)J_{22}$ by the atoms. We assume that the amount of the atomic Stark shift is much smaller than the parameters for CPT: $g^2 a^* a \ll \bar{\Omega}|\Delta_0|$, so that the atoms do not escape from the ground states $|1\rangle$ and $|2\rangle$ even under the perturbation of the cavity field. This weak shift introduces a small detuning to the otherwise resonant two-photon transition between the ground states $|1\rangle$ and $|2\rangle$. Although the otherwise resonant two-photon transition between them is made slightly detuned due to the Stark

shift of the $|2\rangle$ state, the maximal atomic coherence is well maintained, $J_x \approx N$.

In terms of the dark and bright states $|D\rangle$ and $|B\rangle$ in Eq. (5), we write

$$\hat{J}_{22} = \frac{1}{2}(\hat{J}_{DB} + \hat{J}_{DB}^\dagger + \hat{J}_{DD} + \hat{J}_{BB}). \quad (13)$$

Actually, the pair of operators \hat{J}_{DB} and \hat{J}_{DB}^\dagger are the zero mean components orthogonal to the total spin $J_{DD} - J_{BB} = N$ and follow their commutation relation $[\hat{J}_{DB}, \hat{J}_{DB}^\dagger] = N$. This means that the spin ensemble acts as bosons in terms of the superposition states. Then the Hamiltonian (12) for Stark shift takes the form

$$\begin{aligned} \hat{H}_{\text{Stark}} &= -G \hat{a}^\dagger \hat{a} (\hat{J}_{DB} + \hat{J}_{DB}^\dagger + \hat{J}_{DD} + \hat{J}_{BB}) \\ &\quad + i(\varepsilon \hat{a}^\dagger e^{i\Delta_0 t} - \varepsilon^* \hat{a} e^{-i\Delta_0 t}), \end{aligned} \quad (14)$$

where we define the interaction strength $G = g^2/(2\Delta_0)$. The interaction is pictorially depicted in Fig. 1(b). The $-G \hat{a}^\dagger \hat{a} (\hat{J}_{DB} + \hat{J}_{DB}^\dagger)$ term describes the Raman transition between $|D\rangle$ and $|B\rangle$ through $|4\rangle$ (as virtual state) and displays a CPT-based spin \hat{J}_{DB} optodynamics analog to cavity optomechanics [44,50], while the $-G \hat{a}^\dagger \hat{a} (\hat{J}_{DD} + \hat{J}_{BB})$ term describes the transitions from $|D\rangle$ (and $|B\rangle$) through $|4\rangle$ (as the virtual state) back to $|D\rangle$ (and $|B\rangle$) and gives the atomic and field shifts. So far the resonant plus far-off-resonant four-level system is reduced to a resonant three-level one.

Now the simplified three-level system, which is described by Hamiltonians (6) and (14) in terms of the equivalent states ($|D\rangle, |B\rangle, |3\rangle$), serves for our purpose. In Appendix A we derive Heisenberg-Langevin equations in the presence of the Stark shift using the Hamiltonians (6) and (14) and following the standard techniques (as shown in Chap. 12 of [52] and in Chap. 9 in [53]). At the same time we give the steady-state atomic solutions. For the conditions we are interested in for the present scheme (the very weak phase damping $\gamma_z \ll \Gamma_1$ and the weak cavity field $g^2 a^* a \ll \bar{\Omega}|\Delta_0|$), as given in Eqs. (A11) and (A12), Eq. (8) holds. That is, the atoms keep trapped in the dark state. Correspondingly, Eqs. (9) and (11) hold. This establishes the cavity optomechanics analog while the present system keeps its steady-state maximal atomic coherence $J_{12} \approx -N/2$ (i.e., $J_x \approx N$). This lays a foundation for us to explore the coexistence of the spin twisting squeezing with the steady-state maximal atomic coherence.

The essential difference of the present scheme from the optomechanical systems is the coexistence of the spin optomechanics analog [Eq. (14)] with the resonant CPT interaction [Eq. (6)]. This is the very novelty of the present work. It is known that, in cavity optomechanics, there are no resonant interactions involved and there happen only the purely dispersive (far-off-resonant) interactions. Previous schemes for spin squeezing are mainly confined to the far-off-resonant systems to avoid resonant excitation and resonance fluorescence. In sharp contrast, usually the resonant interactions and resonance fluorescence have to be faced within spin systems. Since CPT is a best way to avoid the resonance fluorescence, we expect that CPT resonance-involved spin optodynamics generates spin squeezing. Our purpose is to show that the cavity optomechanics analog manifests its effect in the CPT resonance-based system. In addition, The optomechanical-like interaction $-G \hat{a}^\dagger \hat{a} (\hat{J}_{DB} + \hat{J}_{DB}^\dagger)$ is

accompanied with frequency shift $-G\hat{a}^\dagger\hat{a}(\hat{J}_{DD} + \hat{J}_{BB})$. In contrast, the latter is absent in the optomechanical systems. This leads to the cavity frequency shift $-GN$ and the atomic-state frequency shift $-Ga^*a$. Such shifts will be fed to the ground-state spin that we are interested in and exert their effects on the spin uncertainty. To sum up, what we focus on is not the purely dispersive cavity optomechanics itself but its compatible combination with the CPT resonance.

III. SPIN TWISTING VIA SPIN OPTOMECHANICS ANALOG

Next we make an analytic analysis for the coexistent coherent effects of cavity optomechanics analog and the resonant CPT interaction. In Appendix A we derive a complete set of Heisenberg-Langevin equations [Eq. (A3)] and give the steady-state atomic solutions [Eqs. (A11) and (A12)], $J_{DD} \approx N$, $J_{ij} \approx 0$ ($i, j = D, B, 3; i, j \neq DD$) for the negligible phase damping ($\gamma_z \ll \Gamma_1$) and for the given cavity field ($g^2a^*a \ll \tilde{\Omega}|\Delta_0|$). In this situation we have a self-consistently coupled system for \hat{a} , \hat{J}_{D3} , and \hat{J}_{DB} . We take Heisenberg-Langevin equations from Eq. (A3) as follows:

$$\begin{aligned}\dot{\hat{a}} &= \varepsilon - \left[\frac{\kappa}{2} + i(\Delta_c - G\hat{J}_{DD}) \right] \hat{a} + iG\hat{a}(\hat{J}_{DB} + \hat{J}_{DB}^\dagger) + \hat{F}_a, \\ \dot{\hat{J}}_{D3} &= -[\tilde{\Gamma} + i(\Delta + G\hat{a}^\dagger\hat{a})]\hat{J}_{D3} - i\sqrt{2}\Omega\hat{J}_{DB} + \hat{F}_{J_{D3}}, \\ \dot{\hat{J}}_{DB} &= -\gamma_z(\hat{J}_{DB} - \hat{J}_{DB}^\dagger) - i\sqrt{2}\Omega\hat{J}_{D3} + iG\hat{a}^\dagger\hat{a}(\hat{J}_{DD} - \hat{J}_{BB}) \\ &\quad + \hat{F}_{J_{DB}},\end{aligned}\quad (15)$$

where we define $\tilde{\Gamma} = \Gamma_1 + \gamma_z/2$ as the decay rate for \hat{J}_{D3} , and \hat{F} 's terms are white-noise operators with correlations $\langle \hat{F}_\sigma(t)\hat{F}_\sigma(t') \rangle = 2D_{\sigma\sigma}\delta(t-t')$. The nonzero correlations are derived as $2D_{aa^\dagger} = \kappa$, $2D_{J_{DB}J_{DB}^\dagger} = 2\gamma_zN$, $2D_{J_{DB}J_{DB}} = 2D_{J_{DB}^\dagger J_{DB}^\dagger} = -\gamma_zN$, and $2D_{J_{D3}J_{D3}} = 2\tilde{\Gamma}N$. We write the cavity field as the sum of the mean a ($\neq 0$) and fluctuating parts $\hat{a} = a + \delta\hat{a}$. Since Eq. (8) holds we have $\hat{J}_{ij} \approx \delta\hat{J}_{ij}$. Then Eq. (15) is rewritten

$$\begin{aligned}\delta\dot{\hat{a}} &= -\left(\frac{\kappa}{2} + i\tilde{\Delta}_c \right) \delta\hat{a} + iGa(\hat{J}_{DB} + \hat{J}_{DB}^\dagger) + \hat{F}_a, \\ \dot{\hat{J}}_{D3} &= -(\tilde{\Gamma} + i\tilde{\Delta})\hat{J}_{D3} - i\sqrt{2}\Omega\hat{J}_{DB} + \hat{F}_{J_{D3}}, \\ \dot{\hat{J}}_{DB} &= -\gamma_z(\hat{J}_{DB} - \hat{J}_{DB}^\dagger) - i\sqrt{2}\Omega\hat{J}_{D3} + iGN(a^*\delta\hat{a} + a\delta\hat{a}^\dagger) \\ &\quad + \hat{F}_{J_{DB}},\end{aligned}\quad (16)$$

where we defined $\tilde{\Delta} = \Delta + Ga^*a$ and $\tilde{\Delta}_c = \Delta_c - GN$ as the detunings in the presence of the Stark shift. Since the cavity field noise sideband $\delta\hat{a}$ and the atomic operator \hat{J}_{D3} decays much more rapidly than the ground-state operator \hat{J}_{DB} (i.e., $\tilde{\Gamma}, \kappa \gg \gamma_z$), we can eliminate $\delta\hat{a}$ and \hat{J}_{D3} by setting $\delta\hat{a} = 0$ and $\hat{J}_{D3} = 0$. After doing this we substitute $\delta\hat{a}$ and \hat{J}_{D3} into the equation for \hat{J}_{DB} and give

$$\dot{\hat{J}}_{DB} = -\gamma_z(\hat{J}_{DB} - \hat{J}_{DB}^\dagger) - [\gamma + i(\alpha + \delta)]\hat{J}_{DB} - i\alpha\hat{J}_{DB}^\dagger + \hat{F},\quad (17)$$

where we defined the induced parameters (α, δ, γ) , respectively, as

$$\alpha = -\frac{g^2a^*a}{\Delta_0^2} \frac{2g^2N\tilde{\Delta}_c}{\kappa^2 + 4\tilde{\Delta}_c^2},\quad (18)$$

$$\delta = -\frac{2\Omega^2\tilde{\Delta}}{\tilde{\Gamma}^2 + \tilde{\Delta}^2},\quad (19)$$

$$\gamma = \frac{2\Omega^2\tilde{\Gamma}}{\tilde{\Gamma}^2 + \tilde{\Delta}^2},\quad (20)$$

and the noise $F(t)$

$$\begin{aligned}\hat{F} &= \hat{F}_{J_{DB}} - \frac{i\sqrt{2}\Omega}{\tilde{\Gamma} + i\tilde{\Delta}}\hat{F}_{J_{D3}} \\ &\quad + \frac{ig^2N}{\Delta_0} \left(\frac{a^*}{\kappa + 2i\tilde{\Delta}_c}\hat{F}_a + \frac{a}{\kappa - 2i\tilde{\Delta}_c}\hat{F}_{a^\dagger} \right).\end{aligned}\quad (21)$$

Of these parameters, α appears as both the parametric interaction and the frequency shift, (δ, γ) represent the CPT field-induced frequency shift and decay rate, respectively, and \hat{F} collects the noises from the atomic and the cavity relaxations. From Eq. (17) we can extract the essential mechanism and calculate the spin uncertainty.

We first identify the essential spin optodynamics mechanisms from Eq. (17) before our numerical calculation is presented. Generally, these induced parameters (α, δ, γ) are dependent on the system parameters $(\Delta_0, \tilde{\Delta} = \Delta + g^2a^*a/(2\Delta_0), \tilde{\Delta}_c = \Delta_c - g^2N/(2\Delta_0), \Omega, ga, g^2N, \tilde{\Gamma}, \kappa)$. However, the parametric interaction coefficient α depends on the parameters $(\tilde{\Delta}, \tilde{\Delta}_c, ga, g^2N, \kappa)$, and the relative amplitude of the frequency shift δ to the decay rate γ is determined by the ratio $\tilde{\Delta}/\tilde{\Gamma}$. Therefore, the three induced parameters (α, δ, γ) can be controlled in an independent way. An effective Hamiltonian for the spin interaction is obtained from the coherent terms in Eq. (17) when the relaxation term is temporarily put aside as

$$\hat{H}_{\text{eff}} = (\alpha + \delta)\hat{J}_{DB}^\dagger\hat{J}_{DB} + \frac{\alpha}{2}(\hat{J}_{DB}^2 + \hat{J}_{DB}^{\dagger 2}).\quad (22)$$

Now we can present the spin optodynamics in terms of the Cartesian components of the ground-state spin $(\hat{J}_x, \hat{J}_y, \hat{J}_z)$. Using the definitions in Eq. (10) we express $\hat{J}_{DB} = \frac{1}{2}(\hat{J}_z - i\hat{J}_y)$ and rewrite Hamiltonian (22) as

$$\hat{H}_{\text{eff}} = \frac{\delta}{4}\hat{J}_y^2 + \left(\frac{\alpha}{2} + \frac{\delta}{4} \right) \hat{J}_z^2.\quad (23)$$

Typically, by manipulating the induced parameters (α, δ) we have the standard forms for spin twisting [1,4]

$$\text{OAT: } \hat{H}_{\text{eff}} = \frac{\alpha}{2}\hat{J}_z^2 \quad \text{for } \delta = 0,\quad (24)$$

$$\hat{H}_{\text{eff}} = -\frac{\alpha}{2}\hat{J}_y^2 \quad \text{for } \delta = -2\alpha,$$

and

$$\text{TAT: } \hat{H}_{\text{eff}} = \frac{\alpha}{4}(\hat{J}_z^2 - \hat{J}_y^2) \quad \text{for } \delta = -\alpha.\quad (25)$$

When $\delta = 0$ or $\delta = -2\alpha$, Hamiltonian (23) reduces to the OAT form as in Eq. (24). Alternatively, when $\delta = -\alpha$, the CPT fields and the cavity field induce opposite frequency shifts and combine to give a vanishing shift in total, and thus

Hamiltonian (23) takes the TAT form as in Eq. (25). The conditions for $\delta = -\alpha$ are obtained as

$$\tilde{\Delta}_{\pm} = \frac{1}{\alpha}(\Omega^2 \pm \sqrt{\Omega^4 - \alpha^2 \tilde{\Gamma}^2}), \quad |\alpha| \tilde{\Gamma} \leq \Omega^2, \quad (26)$$

in which the smaller one meets the stability condition [Eq. (36)] as given in the following section. Beyond the above two cases, $\delta \neq (0, -\alpha, -2\alpha)$, the CPT-based spin interaction is in a general twisting form as in Eq. (23).

Before concluding the analytic analysis it is worth recalling the two elements of the present scheme.

The first element is the existence of the CPT resonance for the steady-state maximal atomic coherence. The atoms are prepared in the dark state $|D\rangle$ through the Λ configuration, $J_{DD} = N$. Even when the Stark shift is included, the atoms are almost kept in the dark state, which corresponds to the maximal coherence between the ground states $J_{12} \approx N/2$. In this case we can treat the ensemble of the atoms in terms of the dark state as a bosonized mode \hat{J}_{DB}/\sqrt{N} , which follows the commutation relation $[\hat{J}_{DB}, \hat{J}_{DB}^{\dagger}] \approx N$.

The second element is the existence of the spin optomechanics analog for the spin twisting. When the cavity field is far off resonant with the atoms, $g^2 a^* a \ll \bar{\Omega} |\Delta_0|$, it introduces the Stark shift and preserves the CPT state. The Stark shift behaves as Raman transitions between $|D\rangle$ and $|B\rangle$ and takes an analog of the cavity optomechanics: $-G\hat{a}^{\dagger}\hat{a}(\hat{J}_{DB} + \hat{J}_{DB}^{\dagger})$. The cavity field side-frequency noise responds to the atoms: $\delta\hat{a} = 2iGa(\hat{J}_{DB} + \hat{J}_{DB}^{\dagger})/(\kappa + 2i\tilde{\Delta}_c)$. This gives the spin interaction of the $(\alpha/2)(\hat{J}_{DB} + \hat{J}_{DB}^{\dagger})^2$ form. The feedback is performed through two simultaneous Raman transitions. The simultaneous back-forth transitions lead to a two-order transition: $(\alpha/2)(\hat{J}_{DB}^2 + \hat{J}_{DB}^{\dagger 2})$ and frequency shift $\alpha\hat{J}_{DB}^{\dagger}\hat{J}_{DB}$. Note that this interaction ($\alpha \neq 0$) exists only when $\tilde{\Delta}_c \neq 0$. This is because two degenerate transitions interfere constructively only when $\tilde{\Delta}_c \neq 0$. In fact, the cavity field feeds only its phase back to the atoms just like in the optomechanical case [44]. In addition, due to the CPT resonant interaction, the detuning $\tilde{\Delta}$ and the atomic decay $\tilde{\Gamma}$ are fed to the ground-state spin \hat{J}_{DB} as a frequency shift δ and a relaxation rate γ , respectively, as in Eq. (17).

IV. STEADY-STATE SPIN SQUEEZING

Then we turn to the numerical calculation and check if the spin twisting as in Eqs. (23) to (25) prevails over the atomic and cavity relaxations and yields the steady-state spin squeezing. To obtain an optimized spin uncertainty we use an angle ϕ and define a spin quadrature

$$\hat{J}_{\phi} = \hat{J}_y \cos \phi + \hat{J}_z \sin \phi. \quad (27)$$

Its variance reads

$$\langle \hat{J}_{\phi}^2 \rangle = \langle \hat{J}_y^2 \rangle \cos^2 \phi + \langle \hat{J}_z^2 \rangle \sin^2 \phi + \langle \hat{J}_0^2 \rangle \sin(2\phi), \quad (28)$$

where we defined the cross correlation $\langle \hat{J}_0^2 \rangle = \frac{1}{2}(\langle \hat{J}_z \hat{J}_y + \hat{J}_y \hat{J}_z \rangle)$ and we used $\langle \hat{J}_o^2 \rangle = \langle (\delta \hat{J}_o)^2 \rangle$ ($o = \phi, y, z, 0$) for variances since they have zero means $J_o = 0$. A squeezed spin state is defined as having reduced fluctuations in a certain spin component than a coherent spin state. Spin squeezing happens

when the uncertainty meets the criterion [2,3]

$$\xi^2 = \frac{N \langle \hat{J}_{\phi}^2 \rangle_{\min}}{J^2} < 1. \quad (29)$$

Since we are interested in the weak phase damping ($\gamma_z \ll \Gamma_1$) and the weak cavity field ($g^2 a^* a \ll \bar{\Omega} |\Delta_0|$), as given in Eqs. (A11) and (A12) in Appendix A, Eq. (8) holds, i.e., $J_{DD} \approx N$, $J_{ij} \approx 0$ ($i, j = D, B, 3; ij \neq DD$). From Eq. (10) we have the Cartesian components ($J_x \approx N$, $J_{y,z} \approx 0$), which gives the total spin mean $J \approx J_x \approx N$, and the steady-state maximal atomic coherence $J_{12} \approx -N/2$. As a consequence, the criterion (29) simplifies as

$$\xi^2 = \frac{\langle \hat{J}_{\phi}^2 \rangle_{\min}}{N} < 1. \quad (30)$$

If the criterion is met, the spin twisting squeezing is coexistent with the steady-state maximal atomic coherence. Both of them last so long as the applied fields persist. The smaller the spin uncertainty ξ^2 the stronger the spin squeezing. The angle $\phi = \phi_m$ or $\phi = \pi/2 - \phi_m$ for optimization is found to satisfy

$$\tan(2\phi_m) = \frac{2\langle \hat{J}_0^2 \rangle}{\langle \hat{J}_y^2 \rangle - \langle \hat{J}_z^2 \rangle}. \quad (31)$$

In what follows we perform the calculation from the Heisenberg-Langevin equation (17). For the clearness and conciseness we make a phase shift

$$\hat{J}_{DB} \rightarrow \hat{J}_{DB} e^{i(\frac{\pi}{4} + \frac{\theta}{2})}, \quad (32)$$

with

$$\tan \theta = \frac{\gamma_z}{\alpha}, \quad -\frac{\pi}{2} < \theta < \frac{\pi}{2} \quad (33)$$

and rewrite Eq. (17) in a compact form

$$\dot{\hat{J}}_{DB} = -[\tilde{\gamma} + i(\alpha + \delta)]\hat{J}_{DB} - \tilde{\alpha}\hat{J}_{DB}^{\dagger} + \tilde{F}e^{-i(\frac{\pi}{4} + \frac{\theta}{2})}, \quad (34)$$

where the parameters $(\tilde{\alpha}, \tilde{\gamma})$ are merged with the small quantity γ_z ,

$$\tilde{\gamma} = \gamma + \gamma_z,$$

$$\tilde{\alpha} = \Theta(\alpha)\sqrt{\alpha^2 + \gamma_z^2}, \quad \begin{cases} \Theta(\alpha) = 1 \text{ for } \alpha > 0, \\ \Theta(\alpha) = -1 \text{ for } \alpha < 0. \end{cases} \quad (35)$$

When Ω is comparable to Γ_1 , we have $\tilde{\gamma} \approx \gamma$ since $\gamma_z \ll \Gamma_1$. If $|\alpha|$ is comparable to γ , we also have $\tilde{\alpha} \approx \alpha$. The stability condition, under which the eigenvalues of the drift matrix of both Eq. (34) and its Hermitian conjugate have negative real parts, is derived as

$$\tilde{\gamma}^2 - \tilde{\alpha}^2 + (\alpha + \delta)^2 > 0. \quad (36)$$

Then the set of equations for the coupled correlations is derived

$$\begin{aligned} \frac{d}{dt} \langle \hat{J}_y^2 \rangle &= -2(\tilde{\gamma} - \tilde{\alpha}) \langle \hat{J}_y^2 \rangle + 2(\alpha + \delta) \langle \hat{J}_0^2 \rangle + 2D_1, \\ \frac{d}{dt} \langle \hat{J}_z^2 \rangle &= -2(\tilde{\gamma} + \tilde{\alpha}) \langle \hat{J}_z^2 \rangle - 2(\alpha + \delta) \langle \hat{J}_0^2 \rangle + 2D_2, \\ \frac{d}{dt} \langle \hat{J}_0^2 \rangle &= -2\tilde{\gamma} \langle \hat{J}_0^2 \rangle - (\alpha + \delta)(\langle \hat{J}_y^2 \rangle + \langle \hat{J}_z^2 \rangle) + 2D_0, \end{aligned} \quad (37)$$

where we used the diffusion coefficients

$$\begin{aligned} D_{1,2} &= N[\gamma + \beta + \gamma_z \pm (\beta - \gamma_z) \sin \theta], \\ D_0 &= -N(\beta + \gamma_z) \cos \theta, \end{aligned} \quad (38)$$

and a cavity-loss rate κ involved rate

$$\beta = \frac{g^2 a^* a}{\Delta_0^2} \frac{g^2 N \kappa}{\kappa^2 + 4\tilde{\Delta}_c^2}. \quad (39)$$

By setting $d/dt = 0$ and from Eq. (37) we obtain the variances and cross correlation in steady state as

$$\begin{aligned} \langle \hat{J}_y^2 \rangle &= N \frac{\tilde{\gamma}(\tilde{\gamma} + \tilde{\alpha})[\gamma + \beta + \gamma_z + (\beta - \gamma_z) \sin \theta] + (\alpha + \delta)^2(\gamma + \beta + \gamma_z) - (\tilde{\gamma} + \tilde{\alpha})(\alpha + \delta)(\beta + \gamma_z) \cos \theta}{\tilde{\gamma}[\tilde{\gamma}^2 - \tilde{\alpha}^2 + (\alpha + \delta)^2]}, \\ \langle \hat{J}_z^2 \rangle &= N \frac{\tilde{\gamma}(\tilde{\gamma} - \tilde{\alpha})[\gamma + \beta + \gamma_z - (\beta - \gamma_z) \sin \theta] + (\alpha + \delta)^2(\gamma + \beta + \gamma_z) + (\tilde{\gamma} - \tilde{\alpha})(\alpha + \delta)(\beta + \gamma_z) \cos \theta}{\tilde{\gamma}[\tilde{\gamma}^2 - \tilde{\alpha}^2 + (\alpha + \delta)^2]}, \\ \langle \hat{J}_0^2 \rangle &= N \frac{-(\alpha + \delta)[\tilde{\alpha}\gamma + \tilde{\alpha}(\beta + \gamma_z) + \tilde{\gamma}(\beta - \gamma_z) \sin \theta] - (\tilde{\gamma}^2 - \tilde{\alpha}^2)(\beta + \gamma_z) \cos \theta}{\tilde{\gamma}[\tilde{\gamma}^2 - \tilde{\alpha}^2 + (\alpha + \delta)^2]}. \end{aligned} \quad (40)$$

We analyze the dependence of the parameters on the fields before the numerical results are presented. For vanishing cavity field ($a^*a = 0$, i.e., $\alpha = \beta = 0$) and detuning ($\delta = 0$) and to the first order γ_z/γ we have $\langle \hat{J}_z^2 \rangle \approx N(1 - \gamma_z/\gamma)$, which is very slightly smaller than 1. This is the remaining effect of the ground state phase dephasing in the CPT dark resonance. Since the phasing rate is negligibly small ($\gamma_z \ll \Gamma_1$) and the Rabi frequency is comparable to the decay rate ($\Omega \sim \Gamma_1$), we have $\tilde{\Gamma} \approx \Gamma_1$, $\tilde{\alpha} \approx \alpha$, $\tilde{\gamma} \approx \gamma$. When the parametric interaction strength α is comparable to the rate γ , we have $\theta \rightarrow 0$ ($\sin \theta \rightarrow 0$, $\cos \theta \rightarrow 1$). Thus, the variances are strongly dependent on three kinds of the induced parameters (α ; $\alpha + \delta$; γ , β), as seen from Eq. (40). The first is the twisting interaction strength α , as given in Eq. (18), which is closely related to the cavity detuning $\tilde{\Delta}_c = \Delta_c - g^2 N / (2\Delta_0)$. The second parameter is the total frequency shift $\alpha + \delta$, of which δ is closely related to the atomic detuning $\tilde{\Delta} = \Delta + g^2 a^* a / (2\Delta_0)$. The third kind of parameters are the decay rates (γ , β), which are closely related to the atomic spontaneous emission rate Γ_1 and the cavity loss rate κ , respectively. The parameters (α , β) depend on the original parameters (Δ_0 , $\tilde{\Delta}_c$, $g^2 a^* a$, $g^2 N$, κ) [Eqs. (18) and (39)], while the other parameters (δ , γ) depend on different original parameters (Ω , $\tilde{\Delta}$, $\tilde{\Gamma}$) [Eqs. (19) and (20)]. Therefore, we can manipulate (α , β) and (δ , γ) in an independent way. For a dispersive cavity we are interested in $\kappa \ll 2|\tilde{\Delta}_c|$, we have $\beta \ll |\alpha|$.

For particular parameters we can show the best achievable squeezing. It is seen from Eq. (36) that the stability for the OAT case ($\delta = 0$) is guaranteed for arbitrary α , and the stability for the TAT case ($\alpha + \delta = 0$) is met when $|\alpha| < (\gamma, \Omega^2/\Gamma_1)$. For the sufficiently weak phase damping ($\gamma_z \ll \gamma$) and the dispersive cavity ($\kappa \ll 2|\tilde{\Delta}_c|$), as shown in Appendix B, the steady-state spin uncertainty for OAT and TAT cases is simplified, respectively, as

$$\xi_{\text{OAT}}^2 = 1 - \frac{1}{1 + \sqrt{1 + \gamma^2/\alpha^2}} \quad \text{for } |\alpha| \neq 0, \quad (41)$$

$$\xi_{\text{TAT}}^2 = \frac{1}{1 + |\alpha|/\gamma} \quad \text{for } |\alpha| < (\gamma, \Omega^2/\Gamma_1), \quad (42)$$

both of which are monotonous functions of $|\alpha|/\gamma$. Then we have the same minimal spin uncertainty

$$\xi_{\text{OAT}}^2 \rightarrow \frac{1}{2} \quad \text{for } |\alpha| \gg \gamma, \quad (43)$$

$$\xi_{\text{TAT}}^2 \rightarrow \frac{1}{2} \quad \text{for } |\alpha| \rightarrow \gamma (\leq \Omega^2/\Gamma_1), \quad (44)$$

which indicates the best achievable squeezing of 50% for both OAT and TAT cases. It should be noted that this limit appears generally in steady state and for parametric processes. The twisting interactions behave essentially as optical parametric oscillations, for which the steady-state squeezing has the intrinsic 3-dB limit (50%) due to the detuning and/or instability, as shown in Chap. 16 of [52] and Chap. 7 in [53]. The present case can be shown as follows. Since $\gamma_z \ll \gamma$, we have $\tilde{\alpha} \approx \alpha$, $\tilde{\gamma} \approx \gamma$. From the Langevin equation (17) and the stability condition (36) we can see clearly that the OAT and TAT cases serve as typically different types. For the OAT case ($\delta = 0$), the induced detuning $\alpha + \delta = \alpha$ is the same as the parametric interaction strength α no matter how large it is. It is just the detuning that limits the squeezing. However, for the TAT case ($\delta = -\alpha$), while the induced detuning vanishes $\alpha + \delta = 0$, the induced parametric interaction strength is limited to $|\alpha| < \gamma$ for stability. It is the parametric instability that limits the squeezing. Usually it is the squeezing in the individual frequency components which may be measured by a spectrum analyser based on a homodyne detection scheme. To surpass the limited squeezing, one can use the individual output frequency components which have squeezing beyond 3 dB or even almost perfect squeezing (100%) [43,52–54]. Recently the cavity field feedback [15–18], which is based on the repeated (switchable) and time-dependent atom-cavity-field interactions, serves as a kind of methods to prepare the squeezing beyond 3 dB. Essentially different from this, our scheme is for the steady-state squeezing, which is independent of time. Also the present scheme is different from other methods for the steady-state squeezing such as the quantum state transfer [55,56] and the reservoir engineering [57–59].

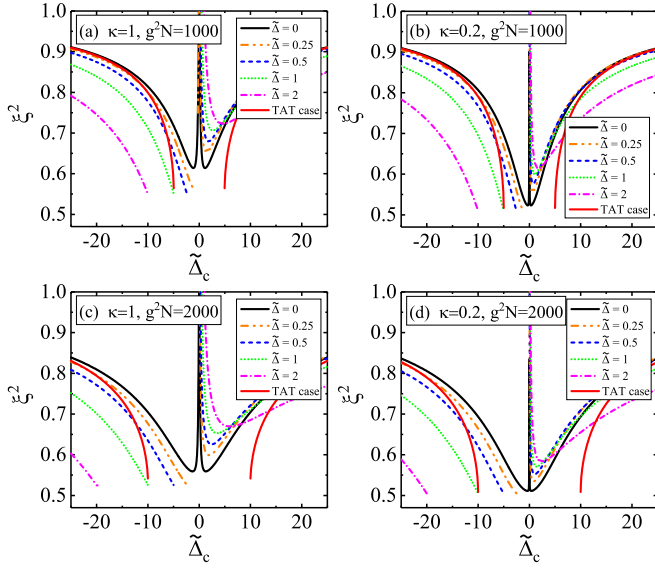


FIG. 2. Spin uncertainty versus the total cavity detuning $\tilde{\Delta}_c$ for different the atomic detunings $\tilde{\Delta} = 0$ (i.e., $\delta = 0$, the OAT case), 0.25, 0.5, 1, 2 and for the TAT case [$\delta = -\alpha$, i.e., $\tilde{\Delta} = \tilde{\Delta}_-$ as in Eq. (26) for the stability]. (a) $\kappa = 1$, $g^2N = 1000$, (b) $\kappa = 0.2$, $g^2N = 1000$, (c) $\kappa = 1$, $g^2N = 2000$, and (d) $\kappa = 0.2$, $g^2N = 2000$. The other parameters are $\Omega = 1$, $ga = 1$, $\Delta_0 = 10$, and $\gamma_z = 10^{-3}$.

To enhance the squeezing if it is necessary, it is feasible to employ the spectral components or the repeated switchable cavity feedback.

We are now in a position to present the numerical dependence of the spin uncertainty on parameters. The atomic decay rates Γ_1 is used as the unit of the decay rates, the Rabi frequencies, the detunings, and the coupling constant. We plot the spin uncertainty ξ^2 versus the total cavity detuning $\tilde{\Delta}_c$ for different atomic detuning $\tilde{\Delta}$ in Fig. 2 and for different parameter g^2N in Fig. 3. It is clearly seen that the spin uncertainty drops below the coherent-state noise level in a very wide range of parameters. This indicates that the spin squeezing appears in such regimes. The best achievable squeezing approaches 50%. The characteristic dependence on the parameters are described as follows.

(i) Two symmetric dips happen about $\tilde{\Delta}_c = 0$ for OAT ($\delta = 0$, i.e., $\tilde{\Delta} = 0$), while two symmetric broken wings appear without a dip for TAT [$\delta = -\alpha$, i.e., $\tilde{\Delta} = \tilde{\Delta}_-$ as in Eq. (26) for the stability]. The first is shown by the black solid lines in Figs. 2(a) and 3(b) in Fig. 3, and the second is shown by the red solid lines in Figs. 2(c) and 2(d) in Fig. 3. The symmetry is because of the exchange between the spin uncertainties $\langle \hat{J}_y^2 \rangle$ and $\langle \hat{J}_z^2 \rangle$ and the invariance of the cross correlation $\langle \hat{J}_0^2 \rangle$ when $\tilde{\Delta}_c$ changes its sign. The OAT case is stable for the whole regime while the TAT case is stable only for the separated two wings.

(ii) Beyond OAT and TAT cases (i.e., for given $\tilde{\Delta}$ but $\delta \neq 0, -\alpha$), two wings are no longer symmetric with respect to $\tilde{\Delta}_c = 0$, and only one wing carries a dip. As shown in the plot, the dip appears when $\tilde{\Delta}_c > 0$. If we switch to $\tilde{\Delta} < 0$ the dip will happen for $\tilde{\Delta}_c < 0$. That is to say, there is an exchange between the left and right sides of the figure when

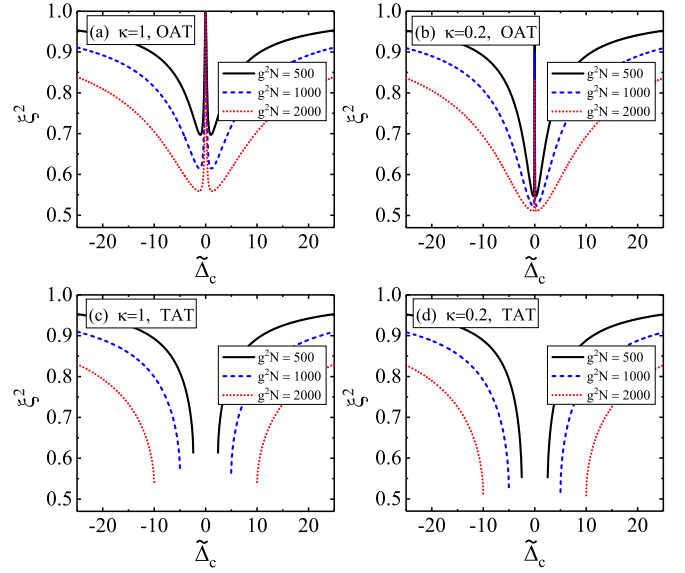


FIG. 3. Spin uncertainty versus the total cavity detuning $\tilde{\Delta}_c$ for different cooperativity parameter g^2N . (a) $\kappa = 1$, (b) $\kappa = 0.2$, for the OAT case ($\delta = 0$, i.e., $\tilde{\Delta} = 0$); and (c) $\kappa = 1$, (d) $\kappa = 0.2$ for the TAT case [$\delta = -\alpha$, i.e., $\tilde{\Delta} = \tilde{\Delta}_-$ as in Eq. (26) for the stability]. The other parameters are the same as in Fig. 2.

$\tilde{\Delta}$ changes its sign. In the disconnected regime the system becomes unstable. As $\tilde{\Delta}$ rises, the two wings are gradually separated from each other.

(iii) The bigger the cooperativity parameter $C = g^2N/(\kappa\Gamma)$ the more the spin uncertainty approaches 0.5, which corresponds 50% squeezing. Although increasing g^2N and decreasing κ are both raise effectively the parameter C , but the two ways have different effects on the wing spread. The case for increasing g^2N is seen from Figs. 2(a) to 2(c) and from Figs. 2(b) to 2(d), and from Figs. 3(c) and 3(d). The case for decreasing κ is shown from Figs. 2(a) to 2(b) and from Figs. 2(c) to 2(d) and in Fig. 3. The two wings spread remarkably as g^2N rises. In comparison, however, the two wings remain almost not spread as the cavity loss rate κ drops. The difference originates from the fact that g^2N appears in the parametric interaction strength α while κ exists only in the diffusion coefficients as the parameter β .

Finally, we give a discussion on the experimental accessibility. Experimentally cold atoms confined in a magneto-optical trap can be used for the present scheme. A great number of atomic structures can be used as candidates. Take ^{87}Rb as an example, the D_1 transition is used for CPT and the D_2 transition serves for the Stark shift, $|1\rangle = |5^2S_{1/2}, F = 1\rangle$, $|2\rangle = |5^2S_{1/2}, F = 2\rangle$, $|3\rangle = |5^2P_{1/2}, F = 1\rangle$, and $|4\rangle = |5^2P_{3/2}, F = 3\rangle$. The cavity parameters of [60] can be used for our purpose, including the beam waist $w \sim 35 \mu\text{m}$, homogeneous laser beams of width $d \sim 50 \mu\text{m}$, and an interaction volume of 10^{-7}cm^3 . An ensemble of $N \sim 10^5$ atoms corresponds to a density of $\lesssim 10^{12} \text{cm}^{-3}$ (small enough to prevent coherence losses due to collisions). For the parameters $g^2N \sim 10^3$ and $\kappa \sim \Gamma_1$, the atom-cavity coupling coefficient is only required to be $g \sim 0.1\Gamma_1$.

TABLE I. Comparison of the present scheme with the previous ones.

Compared aspects	Present scheme	Previous schemes
(1) Coexistence or not of resonant and dispersive interactions	Coexistence of resonant and dispersive interactions (CPT acts as resonant part for steady-state maximal atomic coherence while Stark shift behaves as the dispersive part for spin optomechanics analog and for spin twisting)	No coexistence of resonant and dispersive interactions (Confined to far off resonance regimes after initial preparation of atomic coherence)
(2) Steady-state preparation or time evolution preparation	Steady-state preparation (Spin twisting squeezing and maximal atomic coherence are both prepared in the steady state regardless of initial spin state)	Time evolution preparation (Maximal atomic coherence is initially prepared by microwave pulses and then squeezed spin state is obtained via evolution from initial coherent spin state)

V. CONCLUSION

In conclusion we presented a scheme which combines CPT resonance with the Stark shift. While the first creates the steady-state maximal atomic coherence, the second establishes spin optomechanics analog and yields the spin OAT or TAT (or general twisting between them) interactions. The two coherent effects coexist in a wide range of parameters and last as long as the applied fields persist. Summarized in Table I are the essential differences of the present scheme from the previous ones. The compatible coexistence of CPT with Stark shift provides us with a unique way to exploit the spin optomechanics analog, and to make compatible the spin twisting squeezing with steady-state large or maximal atomic coherence.

ACKNOWLEDGMENTS

This work is supported by the National Natural Science Foundation of China (Grants No. 12274164 and No. 61875067) and the Fundamental Research Funds for the Central Universities (Grant No. CCNU24JC017).

APPENDIX A: HEISENBERG-LANGEVIN EQUATIONS AND ATOMIC STEADY-STATE SOLUTIONS FOR WEAK CAVITY FIELD

The master equation of the atom-cavity system reads as

$$\dot{\hat{\rho}} = -i[\hat{H}, \hat{\rho}] + \Gamma_1 \mathcal{L}_{\hat{J}_{D3}} \hat{\rho} + \Gamma_1 \mathcal{L}_{\hat{J}_{B3}} \hat{\rho} + \gamma_z \mathcal{L}_{\hat{J}_{DB} + \hat{J}_{BD}} \hat{\rho}, \quad (\text{A1})$$

where the system Hamiltonian is written in terms of the dark and bright states and is given by the sum of the CPT part [Eq. (6)] and the Stark shift part [Eq. (14)], i.e.,

$$\hat{H} = \bar{\Omega}(\hat{J}_{B3} + \hat{J}_{3B}) + \Delta \hat{J}_{33} - G \hat{a}^\dagger \hat{a} (\hat{J}_{DB} + \hat{J}_{BD} + \hat{J}_{DD} + \hat{J}_{BB}) + i\varepsilon(\hat{a}^\dagger e^{i\Delta_c t} - \hat{a} e^{-i\Delta_c t}), \quad (\text{A2})$$

and the damping terms take the form $\mathcal{L}_o \hat{\rho} = o \hat{\rho} o^\dagger - \frac{1}{2} o^\dagger o \hat{\rho} - \frac{1}{2} \hat{\rho} o^\dagger o$. Following the standard techniques as in Chap. 12 of [52] and in Chap. 9 in [53]), we derive a complete set of Langevin equation in the rotation frame of the cavity driving

frequency as

$$\begin{aligned} \dot{\hat{a}} &= \varepsilon - \left[\frac{\kappa}{2} + i(\Delta_c - G \hat{J}_{DD}) \right] \hat{a} + iG \hat{a} (\hat{J}_{DB} + \hat{J}_{DB}^\dagger) + \hat{F}_a, \\ \dot{\hat{J}}_{D3} &= -[\tilde{\Gamma} + i(\Delta + G \hat{a}^\dagger \hat{a})] \hat{J}_{D3} - i\bar{\Omega} \hat{J}_{DB} - iG \hat{a}^\dagger \hat{a} \hat{J}_{B3} + \hat{F}_{J_{D3}}, \\ \dot{\hat{J}}_{B3} &= -[\tilde{\Gamma} + i(\Delta + G \hat{a}^\dagger \hat{a})] \hat{J}_{B3} + i\bar{\Omega} (\hat{J}_{33} - \hat{J}_{BB}) \\ &\quad - iG \hat{a}^\dagger \hat{a} \hat{J}_{B3} + \hat{F}_{J_{B3}}, \\ \dot{\hat{J}}_{DB} &= -\gamma_z (\hat{J}_{DB} - \hat{J}_{BD}) - i\bar{\Omega} \hat{J}_{D3} + iG \hat{a}^\dagger \hat{a} (\hat{J}_{DD} - \hat{J}_{BB}) + \hat{F}_{J_{DB}}, \\ \dot{\hat{J}}_{BB} &= \Gamma_1 \hat{J}_{33} + \gamma_z (\hat{J}_{DD} - \hat{J}_{BB}) - i\bar{\Omega} (\hat{J}_{B3} - \hat{J}_{3B}) \\ &\quad - iG \hat{a}^\dagger \hat{a} (\hat{J}_{DB} - \hat{J}_{BD}) + \hat{F}_{J_{BB}}, \\ \dot{\hat{J}}_{DD} &= \Gamma_1 \hat{J}_{33} - \gamma_z (\hat{J}_{DD} - \hat{J}_{BB}) + iG \hat{a}^\dagger \hat{a} (\hat{J}_{DB} - \hat{J}_{BD}) + \hat{F}_{J_{DD}}, \end{aligned} \quad (\text{A3})$$

and those for the Hermitian conjugates if existent. Neglecting the noises \hat{F} 's and factorizing the operators we write simply the equations for the means as

$$\begin{aligned} \dot{J}_{D3} &= -(\tilde{\Gamma} + i\tilde{\Delta}) J_{D3} - i\bar{\Omega} J_{DB} - iG a^* a J_{B3}, \\ \dot{J}_{B3} &= -(\tilde{\Gamma} + i\tilde{\Delta}) J_{B3} + i\bar{\Omega} (J_{33} - J_{BB}) - iG a^* a J_{B3}, \\ \dot{J}_{DB} &= -\gamma_z (J_{DB} - J_{BD}) - i\bar{\Omega} J_{D3} + iG a^* a (J_{DD} - J_{BB}), \\ \dot{J}_{BB} &= \Gamma_1 J_{33} + \gamma_z (J_{DD} - J_{BB}) - i\bar{\Omega} (J_{B3} - J_{3B}) \\ &\quad - iG a^* a (J_{DB} - J_{BD}), \\ \dot{J}_{DD} &= \Gamma_1 J_{33} - \gamma_z (J_{DD} - J_{BB}) + iG a^* a (J_{DB} - J_{BD}), \end{aligned} \quad (\text{A4})$$

with $\tilde{\Gamma} = \Gamma_1 + \gamma_z/2$ and $\tilde{\Delta} = \Delta + G a^* a$. For the weak cavity field $g^2 a^* a \ll \bar{\Omega} |\Delta_0|$ and for the steady state ($\dot{J}_{D3} = \dot{J}_{B3} = 0$) we obtain from the first two equations in Eq. (A4)

$$J_{D3} = \frac{-i\bar{\Omega}}{\tilde{\Gamma} + i\tilde{\Delta}} J_{DB}, \quad J_{B3} = \frac{i\bar{\Omega}}{\tilde{\Gamma} + i\tilde{\Delta}} (J_{33} - J_{BB}). \quad (\text{A5})$$

Then we have $J_{B3} - J_{3B} = \frac{2i\bar{\Omega}\tilde{\Gamma}}{\tilde{\Gamma}^2 + \tilde{\Delta}^2} (J_{33} - J_{BB})$. Using the closure relation $J_{33} + J_{DD} + J_{BB} = N$, we obtain from the last

three equations in Eq. (A4)

$$\begin{aligned}\dot{J}_{DB} &= -\gamma_z(J_{DB} - J_{BD}) - (\gamma + i\delta)J_{DB} + iGa^*a(J_{DD} - J_{BB}), \\ \dot{J}_{BB} &= \Gamma_1(N - J_{DD} - J_{BB}) + \gamma_z(J_{DD} - J_{BB}) \\ &\quad + 2\gamma(N - J_{DD} - 2J_{BB}) - iGa^*a(J_{DB} - J_{BD}), \\ \dot{J}_{DD} &= \Gamma_1(N - J_{DD} - J_{BB}) - \gamma_z(J_{DD} - J_{BB}) \\ &\quad + iGa^*a(J_{DB} - J_{BD}),\end{aligned}\quad (\text{A6})$$

with $\delta = -\frac{\bar{\Omega}^2\bar{\Delta}}{\bar{\Gamma}^2 + \bar{\Delta}^2}$ and $\gamma = \frac{\bar{\Omega}^2\bar{\Gamma}}{\bar{\Gamma}^2 + \bar{\Delta}^2}$. For J_{DB} and J_{BD} we write the equations for $J_{DB} \pm J_{BD}$, respectively,

$$\begin{aligned}\dot{J}_{DB} + \dot{J}_{BD} &= -\gamma(J_{DB} + J_{BD}) - i\delta(J_{DB} - J_{BD}), \\ \dot{J}_{DB} - \dot{J}_{BD} &= -(\gamma + 2\gamma_z)(J_{DB} - J_{BD}) - i\delta(J_{DB} + J_{BD}) \\ &\quad + 2iGa^*a(J_{DD} - J_{BB}).\end{aligned}\quad (\text{A7})$$

We derive the solution of $J_{DB} - J_{BD}$ in the steady state by setting $\dot{J}_{DB} \pm \dot{J}_{BD} = 0$ as

$$J_{DB} - J_{BD} = \frac{2iGa^*a(J_{DD} - J_{BB})}{2\gamma_z + \gamma + \delta^2/\gamma}.\quad (\text{A8})$$

For J_{BB} and J_{DD} we write the equations for $J_{BB} \pm J_{DD}$, respectively,

$$\begin{aligned}(\dot{J}_{BB} + \dot{J}_{DD})/2 &= \Gamma_1(N - J_{DD} - J_{BB}) + \gamma(N - J_{DD} - 2J_{BB}), \\ (\dot{J}_{BB} - \dot{J}_{DD})/2 &= \gamma_z(J_{DD} - J_{BB}) + \gamma(N - J_{DD} - 2J_{BB}) \\ &\quad + 2\lambda(J_{DD} - J_{BB}),\end{aligned}\quad (\text{A9})$$

where $\lambda = \frac{(Ga^*a)^2}{2\gamma_z + \gamma + \delta^2/\gamma}$ describes the population transfer rate due to the cavity field. We derive the solution of J_{DD} in the steady state by setting $\dot{J}_{BB} \pm \dot{J}_{DD} = 0$ as

$$J_{DD} = N \frac{\Gamma_1\gamma + (2\lambda + \gamma_z)(\Gamma_1 + \gamma)}{\Gamma_1\gamma + (2\lambda + \gamma_z)(2\Gamma_1 + 3\gamma)}.\quad (\text{A10})$$

Since $\gamma_z \ll \Gamma_1$ and $g^2a^*a \ll \bar{\Omega}|\Delta_0|$ (which leads to $\lambda \ll \Gamma_1$) we have

$$J_{DD} \approx N.\quad (\text{A11})$$

For the same conditions we have

$$J_{ij} \approx 0 \quad (i, j = D, B, 3; ij \neq DD).\quad (\text{A12})$$

APPENDIX B: SPIN UNCERTAINTY FOR OAT AND TAT SITUATIONS

Here we give the optimized squeezing factors for OAT and TAT situations from Eq. (40). We consider the weak phase

damping ($\gamma_z \ll \gamma$) and the dispersive cavity ($\kappa \ll 2|\tilde{\Delta}_c|$). For the OAT case ($\delta = 0$), it is seen from Eq. (36) that the stability is guaranteed for arbitrary α . The variances and cross correlation in Eq. (40) reduce to

$$\begin{aligned}\langle \hat{f}_{y,z}^2 \rangle &= N \left(1 \pm \frac{|\alpha|}{\gamma} + \frac{\alpha^2}{\gamma^2} \right), \\ \langle \hat{f}_0^2 \rangle &= -N \frac{\alpha|\alpha|}{\gamma^2},\end{aligned}\quad (\text{B1})$$

and then we have the spin uncertainty

$$\begin{aligned}\xi_{\text{OAT}}^2 &= \frac{1}{2N} \left[\langle \hat{f}_y^2 \rangle + \langle \hat{f}_z^2 \rangle - \sqrt{(\langle \hat{f}_y^2 \rangle - \langle \hat{f}_z^2 \rangle)^2 + 4\langle \hat{f}_0^2 \rangle^2} \right] \\ &= 1 - \frac{1}{1 + \sqrt{1 + \gamma^2/\alpha^2}}.\end{aligned}\quad (\text{B2})$$

This is a monotonous function of $\gamma/|\alpha|$ and it takes its values for particular parameters as follows:

$$\xi_{\text{OAT}}^2 = \begin{cases} \rightarrow 1 & \text{for } |\alpha| \ll \gamma, \\ \rightarrow \frac{1}{2} & \text{for } |\alpha| \gg \gamma, \\ \rightarrow 2 - \sqrt{2} & \text{for } |\alpha| = \gamma. \end{cases}\quad (\text{B3})$$

For TAT case ($\delta = -\alpha$), it is seen from Eq. (36) that the stability condition is $|\alpha| \leq \gamma$. The variances in Eq. (40) reduce to

$$\begin{aligned}\langle \hat{f}_{y,z}^2 \rangle &= N \frac{\gamma}{\gamma \mp |\alpha|}, \\ \langle \hat{f}_0^2 \rangle &= 0.\end{aligned}\quad (\text{B4})$$

The spin uncertainty is obtained as

$$\begin{aligned}\xi_{\text{TAT}}^2 &= \frac{1}{N} \langle \hat{f}_z^2 \rangle \\ &= \frac{1}{1 + |\alpha|/\gamma}.\end{aligned}\quad (\text{B5})$$

In the stability range, the spin uncertainty is a monotonous function of $|\alpha|/\gamma$, and it takes its values for particular parameters as follows:

$$\xi_{\text{TAT}}^2 = \begin{cases} \rightarrow 1 & \text{for } |\alpha| \rightarrow 0, \\ \rightarrow \frac{1}{2} & \text{for } |\alpha| \rightarrow \gamma. \end{cases}\quad (\text{B6})$$

- [1] M. Kitagawa and M. Ueda, Squeezed spin states, *Phys. Rev. A* **47**, 5138 (1993).
 [2] D. J. Wineland, J. J. Bollinger, W. M. Itano, F. L. Moore, and D. J. Heinzen, Spin squeezing and reduced quantum noise in spectroscopy, *Phys. Rev. A* **46**, R6797(R) (1992).
 [3] D. J. Wineland, J. J. Bollinger, W. M. Itano, and D. J. Heinzen, Squeezed atomic states and projection noise in spectroscopy, *Phys. Rev. A* **50**, 67 (1994).

- [4] J. Ma, X. Wang, C. P. Sun, and F. Nori, Quantum spin squeezing, *Phys. Rep.* **509**, 89 (2011).
 [5] D. F. Walls and P. Zoller, Enhanced sensitivity of a gravitational wave detector, *Phys. Lett. A* **85**, 118 (1981).
 [6] J. Dunningham and K. Burnett, Sub-shot-noise-limited measurements with Bose-Einstein condensates, *Phys. Rev. A* **70**, 033601 (2004).
 [7] K. Goda, O. Miyakawa, E. E. Mikhailov, S. Saraf, R. Adhikari, K. McKenzie, R. Ward, S. Vass, A. J. Weinstein, and

- N. Mavalvala, A quantum-enhanced prototype gravitational-wave detector, *Nat. Phys.* **4**, 472 (2008).
- [8] L. Amico, R. Fazio, A. Osterloh, and V. Vedral, Entanglement in many-body systems, *Rev. Mod. Phys.* **80**, 517 (2008).
- [9] R. Horodecki, P. Horodecki, M. Horodecki, and K. Horodecki, Quantum entanglement, *Rev. Mod. Phys.* **81**, 865 (2009).
- [10] M. A. Nielsen and I. L. Chuang, *Quantum Computation and Quantum Information* (Cambridge University Press, Cambridge, England, 2000).
- [11] J. Stolze and D. Suter, *Quantum Computing: A Short Course from Theory to Experiment*, 2nd ed. (Wiley-VCH, Weinheim, Germany, 2008).
- [12] A. S. Sørensen and K. Mølmer, Entangling atoms in bad cavities, *Phys. Rev. A* **66**, 022314 (2002).
- [13] T. Fernholz, H. Krauter, K. Jensen, J. F. Sherson, A. S. Sørensen, and E. S. Polzik, Spin squeezing of atomic ensembles via nuclear-electronic spin entanglement, *Phys. Rev. Lett.* **101**, 073601 (2008).
- [14] T. Takano, M. Fuyama, R. Namiki, and Y. Takahashi, Spin squeezing of a cold atomic ensemble with the nuclear spin of one-half, *Phys. Rev. Lett.* **102**, 033601 (2009).
- [15] M. Takeuchi, S. Ichihara, T. Takano, M. Kumakura, T. Yabuzaki, and Y. Takahashi, Spin squeezing via one-axis twisting with coherent light, *Phys. Rev. Lett.* **94**, 023003 (2005).
- [16] M. H. Schleier-Smith, I. D. Leroux, and V. Vuletić, Squeezing the collective spin of a dilute atomic ensemble by cavity feedback, *Phys. Rev. A* **81**, 021804(R) (2010).
- [17] I. D. Leroux, M. H. Schleier-Smith, and V. Vuletić, Implementation of cavity squeezing of a collective atomic spin, *Phys. Rev. Lett.* **104**, 073602 (2010).
- [18] O. Hosten, N. J. Engelsen, R. Krishnakumar, and M. A. Kasevich, Measurement noise 100 times lower than the quantum-projection limit using entangled atoms, *Nature (London)* **529**, 505 (2016).
- [19] C. M. Trail, P. S. Jessen, and I. H. Deutsch, Strongly enhanced spin squeezing via quantum control, *Phys. Rev. Lett.* **105**, 193602 (2010).
- [20] Y. C. Liu, Z. F. Xu, G. R. Jin, and L. You, Spin squeezing: Transforming one-axis twisting into two-axis twisting, *Phys. Rev. Lett.* **107**, 013601 (2011).
- [21] L. I. R. Gil, R. Mukherjee, E. M. Bridge, M. P. A. Jones, and T. Pohl, Spin squeezing in a Rydberg lattice clock, *Phys. Rev. Lett.* **112**, 103601 (2014).
- [22] W. Muessel, H. Strobel, D. Linnemann, D. B. Hume, and M. K. Oberthaler, Scalable spin squeezing for quantum-enhanced magnetometry with Bose-Einstein condensates, *Phys. Rev. Lett.* **113**, 103004 (2014).
- [23] W. Huang, Y. L. Zhang, C. L. Zou, X. B. Zou, and G. C. Guo, Two-axis spin squeezing of two-component Bose-Einstein condensates via continuous driving, *Phys. Rev. A* **91**, 043642 (2015).
- [24] Y. C. Zhang, X.-F. Zhou, X. Zhou, G.-C. Guo, and Z.-W. Zhou, Cavity-assisted single-mode and two-mode spin-squeezed states via phase-locked atom-photon coupling, *Phys. Rev. Lett.* **118**, 083604 (2017).
- [25] J. Borregaard, E. J. Davis, G. S. Bentsen, M. H. Schleier-Smith, and A. S. Sørensen, One-and two-axis squeezing of atomic ensembles in optical cavities, *New J. Phys.* **19**, 093021 (2017).
- [26] M. Wang, W. Qu, P. Li, H. Bao, V. Vuletić, and Y. Xiao, Two-axis-twisting spin squeezing by multipass quantum erasure, *Phys. Rev. A* **96**, 013823 (2017).
- [27] D. D. Yavuz, Single photon SWAP gate using electromagnetically induced transparency, *Phys. Rev. A* **71**, 053816 (2005).
- [28] M. Jain, H. Xia, G. Y. Yin, A. J. Merriam, and S. E. Harris, Efficient nonlinear frequency conversion with maximal atomic coherence, *Phys. Rev. Lett.* **77**, 4326 (1996).
- [29] A. S. Zibrov, M. D. Lukin, L. Hollberg, and M. O. Scully, Efficient frequency up-conversion in resonant coherent media, *Phys. Rev. A* **65**, 051801(R) (2002).
- [30] X. Yang, J. Sheng, U. Khadka, and M. Xiao, Simultaneous control of two four-wave-mixing fields via atomic spin coherence, *Phys. Rev. A* **83**, 063812 (2011).
- [31] H.-T. Tu, K.-Y. Liao, Z.-X. Zhang, X.-H. Liu, S.-Y. Zheng, S.-Z. Yang, X.-D. Zhang, H. Yan, and S.-L. Zhu, High-efficiency coherent microwave-to-optics conversion via off-resonant scattering, *Nat. Photon.* **16**, 291 (2022).
- [32] M. V. Gromovyi, V. I. Romanenko, S. Mieth, T. Halfmann, and L. P. Yatsenko, Storage and retrieval of coherent optical information in atomic populations, *Opt. Commun.* **284**, 5710 (2011).
- [33] E. Arimondo, V coherent population trapping in laser spectroscopy, in *Progress in Optics*, edited by E. Wolf (Elsevier Science, Amsterdam, 1996), Vol. 35, p. 257.
- [34] S. E. Harris, Electromagnetically induced transparency, *Phys. Today* **50**(7), 36 (1997).
- [35] J. P. Marangos, Electromagnetically induced transparency, *J. Mod. Opt.* **45**, 471 (1998).
- [36] M. D. Lukin, Trapping and manipulating photon states in atomic ensembles, *Rev. Mod. Phys.* **75**, 457 (2003).
- [37] M. Fleischhauer, A. Imamoglu, and J. P. Marangos, Electromagnetically induced transparency: Optics in coherent media, *Rev. Mod. Phys.* **77**, 633 (2005).
- [38] O. Kocharovskaya, Amplification and lasing without inversion, *Phys. Rep.* **219**, 175 (1992).
- [39] M. O. Scully, From lasers and masers to phaseonium and phasers, *Phys. Rep.* **219**, 191 (1992).
- [40] P. Mandel, Lasing without inversion: A useful concept? *Contemp. Phys.* **34**, 235 (1994).
- [41] J. Mompert and R. Corbalán, Lasing without inversion, *J. Opt. B: Quantum Semiclassical Opt.* **2**, R7 (2000).
- [42] M. O. Scully and M. Fleischhauer, High-sensitivity magnetometer based on index-enhanced media, *Phys. Rev. Lett.* **69**, 1360 (1992).
- [43] A. Dantan, J. Cviklinski, E. Giacobino, and M. Pinar, Spin squeezing and light entanglement in coherent population trapping, *Phys. Rev. Lett.* **97**, 023605 (2006).
- [44] M. Aspelmeyer, T. J. Kippenberg, and F. Marquardt, Cavity optomechanics, *Rev. Mod. Phys.* **86**, 1391 (2014).
- [45] C. Fabre, M. Pinar, S. Bourzeix, A. Heidmann, E. Giacobino, and S. Reynaud, Quantum-noise reduction using a cavity with a movable mirror, *Phys. Rev. A* **49**, 1337 (1994); S. Mancini, and P. Tombesi, Quantum noise reduction by radiation pressure, *ibid.* **49**, 4055 (1994).
- [46] V. Braginskii and F. Y. Khalili, *Quantum Measurement* (Cambridge University Press, Cambridge, England, 1995).
- [47] S. Gigan, H. R. Böhm, M. Paternostro, F. Blaser, G. Langer, J. B. Hertzberg, K. C. Schwab, D. Bäuerle, M. Aspelmeyer,

- and A. Zeilinger, Self-cooling of a micromirror by radiation pressure, *Nature (London)* **444**, 67 (2006).
- [48] D. Vitali, S. Gigan, A. Ferreira, H. R. Böhm, P. Tombesi, A. Guerreiro, V. Vedral, A. Zeilinger, and M. Aspelmeyer, Optomechanical entanglement between a movable mirror and a cavity field, *Phys. Rev. Lett.* **98**, 030405 (2007).
- [49] K. W. Murch, K. L. Moore, S. Gupta, and D. M. Stamper-Kurn, Observation of quantum-measurement backaction with an ultracold atomic gas, *Nat. Phys.* **4**, 561 (2008).
- [50] N. Brahms and D. M. Stamper-Kurn, Spin optodynamics analog of cavity optomechanics, *Phys. Rev. A* **82**, 041804(R) (2010).
- [51] T. Holstein and H. Primakoff, Field dependence of the intrinsic domain magnetization of a ferromagnet, *Phys. Rev.* **58**, 1098 (1940).
- [52] M. O. Scully and M. S. Zubairy, *Quantum Optics* (Cambridge University Press, Cambridge, England, 1997).
- [53] D. F. Walls and G. J. Milburn, *Quantum Optics* (Springer, Berlin, 1994).
- [54] R. Guzmán, J. C. Retamal, E. Solano, and N. Zagury, Field squeeze operators in optical cavities with atomic ensembles, *Phys. Rev. Lett.* **96**, 010502 (2006).
- [55] J. Hald, J. L. Sørensen, C. Schori, and E. S. Polzik, Spin squeezed atoms: A macroscopic entangled ensemble created by light, *Phys. Rev. Lett.* **83**, 1319 (1999).
- [56] A. Dantan and M. Pinard, Quantum-state transfer between fields and atoms in electromagnetically induced transparency, *Phys. Rev. A* **69**, 043810 (2004).
- [57] E. G. Dalla Torre, J. Otterbach, E. Demler, V. Vuletic, and M. D. Lukin, Dissipative preparation of spin squeezed atomic ensembles in a steady state, *Phys. Rev. Lett.* **110**, 120402 (2013).
- [58] X.-M. Hu, Entanglement generation by dissipation in or beyond dark resonances, *Phys. Rev. A* **92**, 022329 (2015).
- [59] S.-Y. Bai and J.-H. An, Generating stable spin squeezing by squeezed-reservoir engineering, *Phys. Rev. Lett.* **127**, 083602 (2021).
- [60] M. Hennrich, T. Legero, A. Kuhn, and G. Rempe, Vacuum-Stimulated raman scattering based on adiabatic passage in a high-finesse optical cavity, *Phys. Rev. Lett.* **85**, 4872 (2000).